ORIGINAL ARTICLE

Water uptake of radiata pine wood after microwave and superheated steam treatments: sapwood vs. heartwood

Huimin Cao[1,2] · Saisai Huang[1] · Fangyu Yin[1] · Yufa Gao[1] · Xiaomei Liao[1] · Songlin Yi[2] · Yongdong Zhou[1]

Abstract

Resin canals and ray cells in pine wood connect the interior to the exterior. The blockage of resin canals and ray cells by the resin, directly determines the water uptake of the wood. However, research on water uptake by resinous wood is lacking. Hence, this study aimed to explain how microwave (MW) or superheated steam (SS) treatment improves wood water uptake from the perspective of resin content (RC). Therefore, radiata pine sapwood and heartwood were treated with MW, SS, or microwave-superheated steam (MS) for different times. The results showed that MW and SS treatments expelled the internal resin of radiata pine. Owing to the low RC and high moisture content (MC) of sapwood, the effect of the MW treatment on the RC of radiata sapwood was insignificant. Heartwood has a markedly higher RC and lower MC than sapwood; therefore, MW treatment can drive part of the resin to migrate out of the wood. With increasing SS treatment time, the RC of the sapwood and heartwood decreased to varying degrees; however, the core layer resin could not be completely removed. In addition, MW treatment can accelerate the degreasing process as it discharges some part of the resin and opens some parts of the resin canals. Moreover, MS treatment can increase the porosity of sapwood and heartwood due to the expulsion of resin. MS treatment had no significant effect on sapwood water uptake; however, it increased that of heartwood by more than three times. The dye solution enters the wood through the open resin canals or ray cells and communicates with the axial resin canals. Therefore, the water uptake of heartwood is mainly related to the resin content and the blockage of the resin canals by the resin determines the entry of the dye solution to the interior of the wood.

1 Introduction

Radiata pine (*Pinus radiata D. Don*) is a highly domesticated pine owing to its characteristics such as: easy reproduction, rapid growth, controllable pests and diseases, acceptable wood quality, and economic benefits (Wu 2019). In countries such as New Zealand, Australia, and Chile, large-scale plantations can meet domestic needs and gain commercial value. Therefore, radiata pine has become an effective substitute for various woods that can be used in construction, furniture, and papermaking (Benedetti et al. 2019; Dong et al. 2020; Srinivasan et al. 2007). However, radiata pine must be impregnated to improve its durability prior to its use as a building material or outdoor product (Aguayo et al. 2021; Andeme Ela et al. 2021; Torgovnikov and Vinden 2010). Moreover, the entry of preservatives in the interior of wood is critical (Nguyen et al. 2013). However, obtaining a satisfactory impregnation effect for radiata pine with a high resin content (RC) is difficult, as the resin may clog resin canals, ray cells, and pits (Matsumura et al. 1998, 1999). Therefore, improving the permeability of resinous wood can effectively enhance the impregnation of preservatives and yield high-quality wood products.

✉ Yongdong Zhou
zhouyd@caf.ac.cn

1 Research Institute of Wood Industry, Chinese Academy of Forestry, Beijing 100091, PR China

2 College of Material Science and Technology, Beijing Forestry University, Beijing 100083, PR China

Permeability is the ability of a fluid to enter or pass through a material (Mahdian et al. 2020). Although wood is porous, the permeabilities of different tree species vary considerably because of their complex structures. Heartwood and sapwood permeabilities differ even though they belong to the same tree species; this is influenced by the resin or sediment (Bailey and Preston 1969; Belt et al. 2017). In particular, liquid permeability is affected by liquid viscosity, molecular size, and liquid-wood interactions. Wood is also used as a porous material for wastewater treatment and seawater desalination (Chen et al. 2017; He et al. 2019; Jiang et al. 2018). Therefore, dyes, modifiers, and preservatives cannot easily enter the wood interior because of the filtering effect of porous materials. The opening of large pores in wood, such as ray cells and resin canals, determines whether dyes, modifiers, or preservatives can quickly enter the wood interior.

Many studies have been conducted on wood permeability, including measurements of the longitudinal and radial permeability of wood and the reasons for the differences in permeability (Ai et al. 2017; Ananías et al. 2022; Mahdian et al. 2020; Pokki et al. 2010a, b; Tan et al. 2020). Research on improving wood permeability mainly includes steam explosion, microwave (MW) treatment, ultrasonic treatment, heat treatment, bioincising, and cooking (Eliseev et al. 2022; Fang et al. 2023; Jang and Kang 2019, 2023; Kang et al. 2021; Pokki et al. 2010a, b; Qian et al. 2022). Among them, many have reported that MW treatment improves wood permeability (Eliseev et al. 2022; Torgovnikov and Vinden 2010; Weng et al. 2020; Zhang et al. 2021); this involved different equipment, power, and tree species. Overall, the MW radiation caused polar molecules, particularly water molecules, inside the wood to vibrate, instantaneously generating excessive amounts of heat (Singh et al. 2016), thereby generating steam pressure inside the wood and causing steam to escape, breaking through pits, parenchyma, and resin canals. In addition, it can cause rupture of the wood structure and some macro- and microcracks may form (Ganguly et al. 2021). High-intensity MW can make wood several times more permeable, providing favourable conditions for wood drying and functional utilisation (Torgovnikov and Vinden 2010). In addition, drying methods affect wood permeability (Taghiyari et al. 2014). Among them, superheated steam (SS) drying improves wood permeability because temperatures > 100 °C cause steam pressure to develop inside the wood (Pakowski et al. 2009), which may open aspirated pits or destroy pit membranes.

The effects of MW and SS on wood permeability have been extensively studied. However, few studies have combined these two technologies, and they are not specific to resinous wood. In addition, previous MW treatment studies improved wood permeability by creating gaps (Vinden et al. 2011; Zhang et al. 2021), which may greatly reduce wood strength and limit its application in certain fields. Some studies have also shown that mild MW treatment can destroy the pit membrane structure but cannot significantly increase the permeability or water diffusion coefficient (Beikircher et al. 2012; Li et al. 2005). This indicates that the improvement in wood permeability depends on pore size. Therefore, research is scarce on improving the permeability of wood without macroscopic cracks. Considering that the ray cells or resin canals in pine are channels that connect the interior and exterior of the wood (Arbellay et al. 2014; Bannan 1936), it is easier for the liquid to soak into the wood from these tissues. Therefore, blocking the ray cells and the transverse resin canal has an important impact on the transverse permeability of wood. However, most studies have focused on destroying pits and parenchymal cells rather than blocking resin canals or ray cells. For resinous wood, opening the resin canals may increase the permeability of the wood rather than destroying its original structure. The temperature of SS treatment exceeds 100 °C, which can promote resin migration and open blocked resin canals. However, there is a lack of research on using SS to improve the permeability of resinous wood.

Therefore, this study investigated the effect of resin removal on radial water uptake by radiata pine sapwood and heartwood. Hence, radiata pine wood was treated with MW, SS, and microwave-superheated steam (MS), and the blockage of the resin canals, RC, porosity, and water uptake were analysed to reveal the reasons for the increase in water uptake. Moreover, the potential of MS treatment of coniferous wood has been demonstrated.

2 Materials and methods

2.1 Materials and sample preparation

Radiata pine with a diameter of 500 mm was obtained from New Zealand. After felling without any treatment, it was transported to Shandong, China, and shipped to the laboratory. Before the experiment, the logs were sawn into lumber samples with dimensions of 2500 mm × 50 mm × 20 mm (L × T × R), and all samples were obtained from the same log. The samples were divided into heartwood and sapwood groups, with three samples selected for each group. These samples did not contain a pith, heart-sapwood junction zone, or near bark. The 20 mm thick planks were selected because they are commonly used for outdoor fences or floors and are easy to impregnate under laboratory conditions. The planks were divided into four sections, and a 10 mm thick test piece was used to test the moisture content (MC) and RC (Fig. 1). The samples labelled 'A' were regarded as the
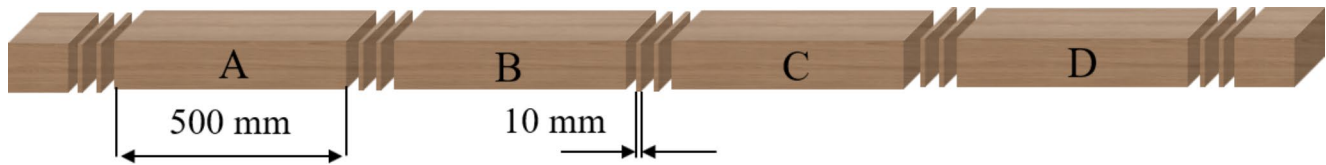
Fig. 1 Diagram of Wood segmentation

Table 1 MW treatment process design

Group	Power (kW)	Processing time(s)	Energy density (kWh/m³)
MW-40s	18	40	100
MW-60s	18	60	150
MW-80s	18	80	200

Table 2 Superheated steam process design

Group	Temperature (°C)	Oxygen concentration (%)	Time (h)
SS-3 h	110	2	3
SS-6 h	110	2	6
SS-9 h	110	2	9
MS-3 h	110	2	3
MS-6 h	110	2	6
MS-9 h	110	2	9

control materials and equilibrated in a constant temperature and humidity chamber at 20 °C/65% relative humidity (RH). Samples labelled 'B', 'C', and 'D' were subjected to MW, SS, and MS treatments, and three replicates were set up for each group of samples.

The MC test piece was dried at 103 ± 2 °C to determine the initial MC of the wood. The MC was calculated using Eq. 1:

$$MC = (M_0 - M_1) / M_1 \times 100\% \tag{1}$$

where M_0 and M_1 represent the initial and oven-dried wood weights, respectively.

The samples were weighed before and after MW, SS, and MS treatments to determine their final MC. After the MW, SS, and MS treatments, the samples were equilibrated in a constant temperature and humidity chamber at 20 °C/65% RH for subsequent detection.

2.2 Microwave treatment

MW equipment (WX20L-19, Sanle, Nanjing, China) with a feed unit was used for wood treatment. The equipment was rated at 20 kW and operated at 0.915 GHz, with the feed rate determining the processing time. According to previous experimental results, the energy density of MW is determined by the power and processing time. When the energy density is the same, a higher power and shorter treatment time are beneficial for improving the permeability of wood; however, the generation of defects must be avoided. Therefore, the maximum power allowed by the equipment (18 kW) was selected, and three processing times were used in this study. The specific process is shown in Table 1.

2.3 Superheated steam treatment

The SS treatment test was performed using self-designed high-temperature drying test equipment. The equipment was equipped with air circulation and oxygen concentration control systems. The oxygen concentration could be regulated by the water vapour concentration. A low-oxygen environment provided by a high concentration of water vapour can reduce the oxidation reaction of wood. The test was conducted at atmospheric pressure and performed in accordance with Table 2, and a 1 h preheating process at 90 °C was conducted before formal processing. In addition, according to the MW experimental results, the MW-60s samples were used for subsequent SS treatment since some MW-80s samples were deformed, which may be due to the long treatment time, and the MW-40s sample may not have achieved the best treatment effect. The SS treatment temperature was determined based on the SS drying process and the melting point of rosin. As the melting point of rosin is 110 to 135 °C, a drying process at 110 °C was performed in this study.

2.4 Morphological characteristics

Specimens with dimensions of 5 mm × 5 mm × 5 mm (L × T × R) were obtained from the control, MW, SS, and MS treated samples. Flat cross sections and tangential sections were obtained using a microtome. The MW, SS, and MS treatment samples included surface and core layer samples, which were procured 10 mm away from the surface. The resin canal and morphology were observed using a simple extended depth-of-field 3D microscope (VHX-6000, KEYENCE, Osaka, Japan).

2.5 Resin extraction

Three pieces of 15 mm long samples were cut from each sample for resin extraction. Samples treated with MW, SS, and MS were first prepared to remove the surface resin. The samples were first divided into thin slices with a thickness of 1–2 mm and dried in a vacuum drying oven (40 °C, 5 kPa) with a built-in desiccant to a constant weight as the oven dry weight. The wood chips from each sample were weighed to the nearest 0.001 g. The resin was extracted by ethanol soaking according to the method of Matsumura et al. (1999); however, the temperature was set to 60 °C to accelerate the extraction. Wood chips were added to a 100 mL beaker, 70 mL of absolute ethanol was added, and the mixture was sealed with a plastic film. A constant temperature water bath was set at 60 °C as the extraction condition for this experiment; the time lasted for 48 h, during which the ethanol solvent was replaced once. After the experiment, the samples were washed in ethanol solvent at 60 °C to remove residual resin. After volatilising the residual alcohol at room temperature, the sample was vacuum-dried and weighed. The RC is the mass difference after extraction with ethanol divided by the initial mass of the sample. The RC was calculated using Eq. 2:

$$RC = (R_0 - R_1)/R_0 \times 100\% \tag{2}$$

where R_0 is the weight of the sample before extraction, and R_1 is the weight after extraction.

2.6 Porosity and pore size distribution analysis

For porosity testing, specimens, 6 mm × 10 mm × 10 mm (L × T × R), were taken from the control and MS-9 h-treated samples, including earlywood and latewood. Before the experiment, the specimens were vacuum-dried (40 °C, 5 kPa) to remove moisture. Porosity tests were performed using an automatic mercury porosimeter (AutoPore IV 9510, Micromeritics, GA, USA). The specimen was placed in a penetrometer, and pressure was applied to force mercury into the specimen. The maximum intrusion pressure was 227 MPa, the surface tension and contact angle were determined according to Weng et al. (2020), and the pore size distribution was determined using the Washburn equation (Washburn 1921).

2.7 Impregnation

The control, MW, SS, and MS samples, three samples each group, were prepared and cut into 50 mm long samples for vacuum impregnation to test the water uptake of the samples. In this study, only the change in water uptake of the tangential section was investigated. This is because liquid absorption mainly occurs in the axial and tangential directions (Matsumura et al. 1998). This study aimed to explore the effect of transverse resin canal blockage on wood water uptake. Therefore, the specimens were sealed with epoxy resin, except for the two tangential sections. The samples were soaked in an aqueous solution of toluidine blue (0.1 wt%) in a beaker and weight-loaded with stainless-steel blocks, and the bottom and upper parts were separated using stickers. The beaker was immersed in a vacuum chamber at 20 kPa; the sapwood and heartwood were treated for 10 and 20 min, respectively. The pressure was then slowly released and allowed to stand for 2 min. After impregnation, the dye solution on the wood surface was wiped off with an absorbent paper, the sample was weighed, the volume was measured, and the uptake was calculated. This study used vacuum impregnation as it is easier to perform in a laboratory. A shorter treatment time is required to better observe the penetration path of the dye solution and avoid diffusion of the dye solution into the tracheids by long-term impregnation. In addition, it is necessary to obtain an easier path for the liquids to enter.

The impregnated samples were cut and photographed to observe the dye penetration. Tangential and cross sections of the MS-9 h samples were also prepared, and the flow paths of the dye solution were observed under an extended depth-of-field 3D microscope.

2.8 Data analysis

Microsoft Excel (Microsoft, WA, USA) was used for the t-test; when $p < 0.05$, a significant difference was observed between the two sets of data; and a, b, c, and d were used to indicate whether each set of data was significantly different from the previous set.

3 Results and discussion

3.1 Wood moisture content changes

The green MC of radiata pine sapwood and heartwood differs considerably; the green MC range of sapwood is 80–100%, and that of heartwood is approximately 30%. The MC of the radiata pine wood before and after MW, SS, and MS treatment are shown in Fig. 2. MW can reduce the MC of wood; under the same power, the longer the treatment time, the lower the MC. In the experiment, 18 kW treatment for 80 s easily deformed the wood; therefore, the subsequent process of 18 kW treatment for 60 s was adopted. Under SS conditions, the MC of wood decreased rapidly, and those of heartwood and sapwood decreased to different
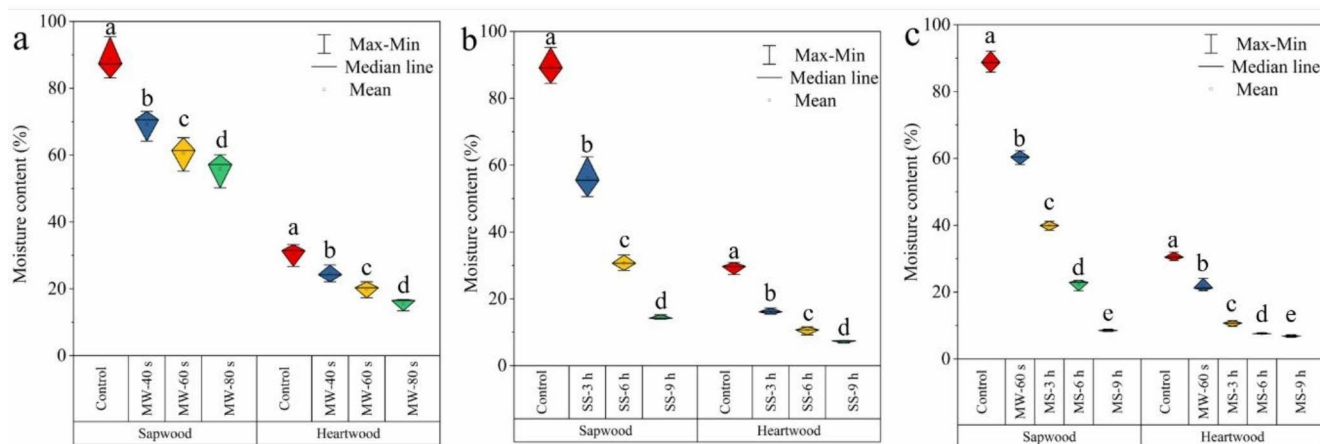
Fig. 2 Moisture content of sapwood and heartwood before and after MW (**a**), SS (**b**), and MS (**c**) treatments
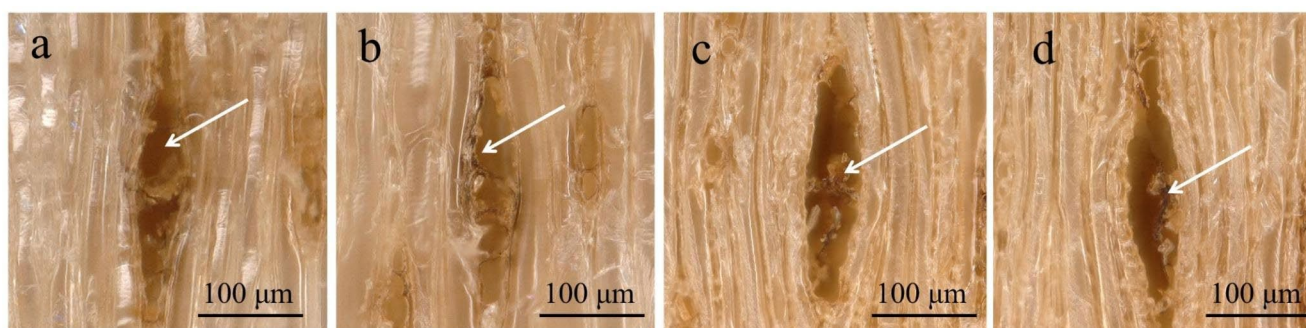Note: control is green wood moisture content

Fig. 3 Microscopic image of sapwood core layer. (**a**) control; (**b**) MW-60s; (**c**) SS-9 h; (**d**) MS-9 h. The arrows point to the voids (**a**) or the resin (**b**, **c**, and **d**) of the resin canals

extents with prolonged treatment time. The mean MC of the sapwood decreased by 33.6%, 59.1%, and 74.9% after 3 h, 6 h, and 9 h, respectively, whereas that of the heartwood decreased by 13.2%, 18.8%, and 22.2%, respectively. As shown in Fig. 2c, MW can accelerate the drying process of SS, and the MC of the MS samples was lower than that of the SS samples for the same treatment time as MW treatment reduces the MC of the wood and the MW treatment can open the pathway from the interior to the exterior of the wood, accelerating its drying process (Weng et al. 2021).

3.2 Morphological observation of resin in resin canal

Figure 3 shows microscopic images of the tangential sections of the sapwood control, MW-60s, SS-9 h, and MS-9 h samples. The micromorphologies of the resin canals in the core and surface layers of the sapwood were similar, and only the micro-images of the core layer are provided here. The amount of resin in the sapwood resin canals was lower and voids were still present in the resin canals (Fig. 3a). After MW treatment, there was no resin exudation on the wood surface, and there was no significant change in the resin canals; however, resin shrinkage was visible (Fig. 3b), which may have been caused by the loss of volatile components in resin, as high temperatures can volatilize the turpentine in the resin (Hawley and Palmer 1912; Potter and Schuerch 1975). Similar results were observed for the SS-9 h and MS-9 h samples, in which resin shrinkage and ray parenchyma cells were dissected (Fig. 3c, d). In addition, the resin in the uniseriate ray cells of the sapwood is almost invisible.

Figure 4 shows microscopic images of the tangential surfaces of the control, MW-60s, and SS-3 h heartwood samples. After the MW or SS treatment, part of the wood surface was covered with resin (Fig. 4b, c). This shows that heartwood contains a large amount of resin, and after MW or SS treatment, the resin inside the wood seeps out to the wood surface. This indicates that MW and SS are effective resin removal methods.

Figure 5 shows a microscopic image of the transverse resin canals and uniseriate ray cells in the tangential section of the heartwood control, MW-60s, and MS-9 h samples. The SS-treated samples were similar to the MS-treated samples

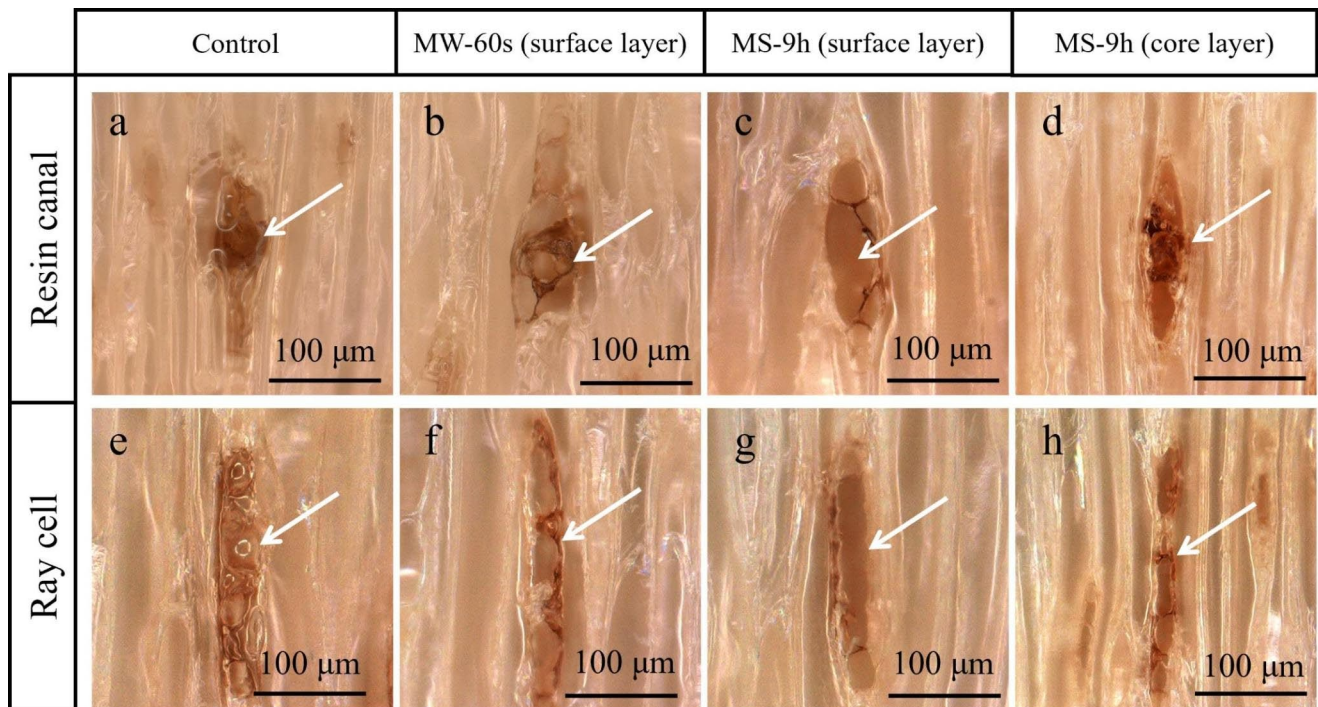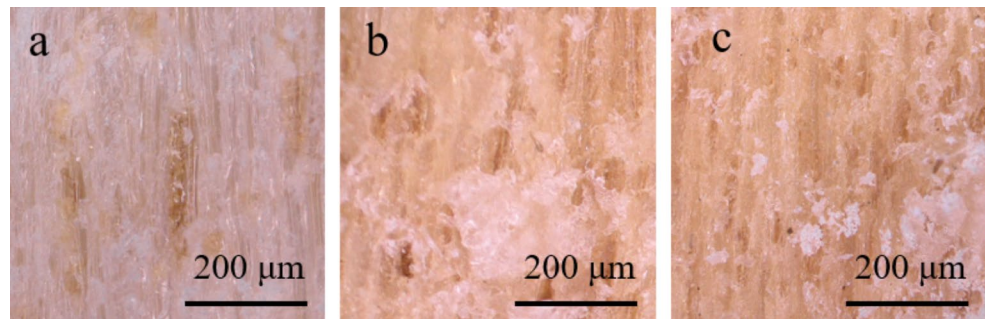**Fig. 4** Microscopic image of heartwood surface. (**a**) control; (**b**) MW-60s; (**c**) SS-3 h

Fig. 5 Microscopic image of heartwood tangential section. The arrows points to the resin (**a**, **b**, **d**, **e**, **f**, and **h**) or voids (**c** and **g**) of the resin canals or ray cells

and are not presented separately here. The heartwood resin canals were almost fully filled with resin (Fig. 5a), and some ray cells were filled with resin (Fig. 5e). After MW treatment, some voids were found inside the resin canals or ray cells in the surface layer, and the resin shrank (Fig. 5b, f). This phenomenon was aggravated after MS treatment, and the destruction of some parenchymal cells was visible (Fig. 5c, g). This shows that the turpentine evaporation and resin discharge were intense, and the blocked resin canals or ray cells were opened. However, the core layer contained more resin attached to the inner walls of the resin canals (Fig. 5d, h). This indicates that the resin inside the inner heartwood was not completely removed.

Figure 6 shows the cross-sectional microscopic images of the heartwood before and after MS treatment. The axial resin canal of the control sample was filled with resin (Fig. 6a). This may have been due to cutting during sample preparation, which could have caused the resin in the epithelial cells to flow into the resin canals. The amount of resin inside the axial resin canals was significantly reduced after MS treatment, and holes appeared in the resin canals (Fig. 6c). In addition, the resin morphology of the latewood bands changed significantly. Some of the tracheids in the latewood zone of the untreated wood were filled with resin (Fig. 6b). However, this phenomenon disappeared in the MS-treated samples, and only some resin was attached to the tracheid wall (Fig. 6d). Additionally, the amount of resin in some radial resin canals and ray cells was significantly reduced (Fig. 6d).

3.3 Resin content

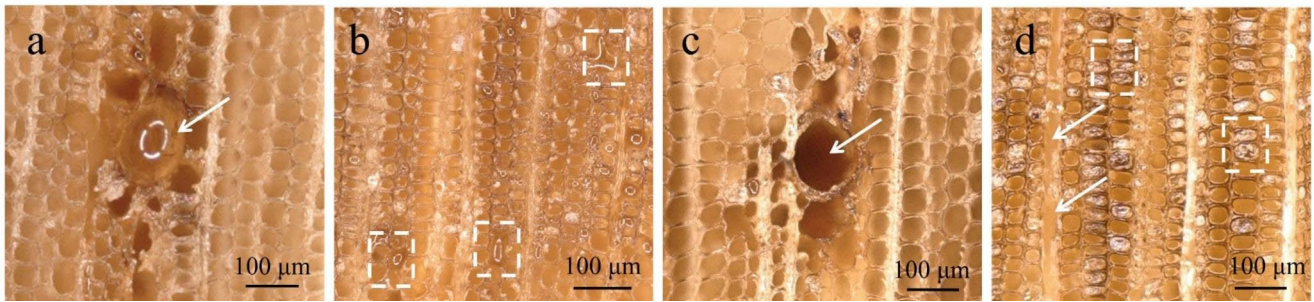Figure 7 shows the RC of the wood before and after the MW, SS, and MS treatments. The MW treatment had a negligible

Fig. 6 Microscopic image of heartwood cross-section of control (**a**, **b**) and MS-9 h (**c**, **d**) sample. The arrows point to the resin (**a**) and voids (**c** and **d**) of the resin canals or ray cells; the wireframes contain the characteristics of the resin inside the tracheid (**b** and **d**)
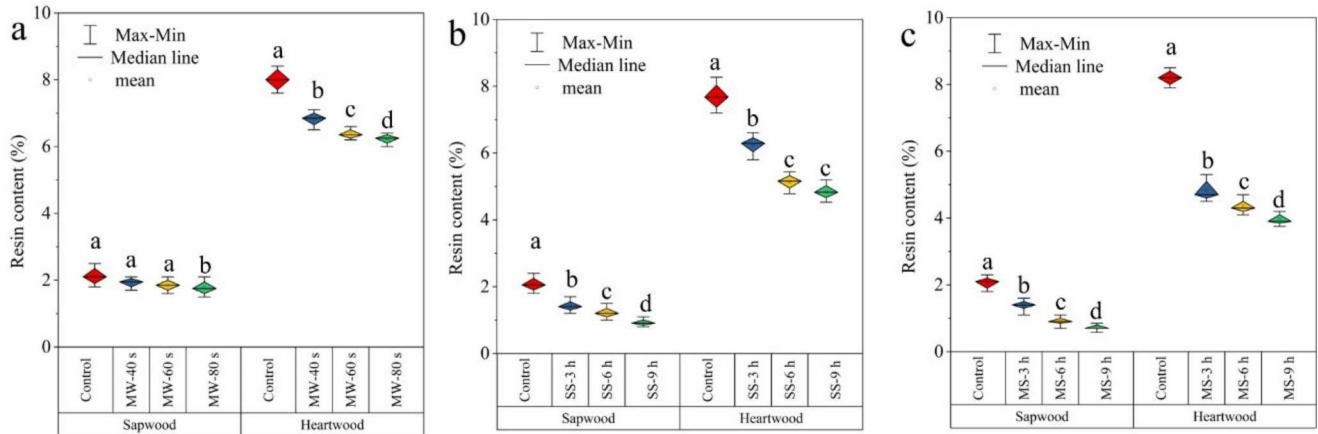

Fig. 7 Resin content of sapwood and heartwood before and after MW (**a**), SS (**b**), and MS (**c**) treatments

effect on the RC of the sapwood (Fig. 7a). The RC of the group treated at 18 kW for 80 s was slightly reduced; however, there was no significant difference compared to that of the other groups. This may be due to the low RC in the sapwood, and only part of the turpentine volatilised with water vapour during the MW treatment. Therefore, there was little difference in the RC before and after MW treatment. The microscopic image in Fig. 3 confirms that only a small amount of resin was present in the sapwood resin canal. The MW treatment had a greater effect on the RC of heartwood (Fig. 7a). The RC of the three groups was significantly reduced after MW treatment.

The SS treatment had a significant effect on the RC of sapwood and heartwood. For sapwood, treatments for 3 h, 6 h, and 9 h reduced the average RC by 1.4%, 1.2%, and 0.9%, respectively. This may be due to the longer treatment time of SS and more resin being carried out during the volatilisation of wood moisture. For heartwood, turpentine volatilised, and a large amount of liquid resin moved from the interior to the wood surface (Fig. 4c). Therefore, the RC decreased further, and as the treatment time increased, the RC gradually decreased.

As shown in Fig. 7c, MW treatment accelerates the discharge of the resin. Compared with the SS treatment, the

RC of the MS samples was lower for the same treatment time, since MW treatment can discharge part of the resin and reduce the RC. The MW treatment may also open partially closed pores, which are conducive to the movement of the resin. In addition, the planing treatment after MW treatment removed the surface resin, which was beneficial for discharging the resin during the subsequent SS treatment. However, the average final RC of sapwood was 0.7%, and that of heartwood was 3.9%. This shows that under the conditions of this experiment, the MS treatment could not completely remove the resin from the wood. As shown in Fig. 5d, a large amount of resin remains in the resin canals inside the wood. This is because the resin becomes more viscous and less fluid as drying progresses. Therefore, the pine resin inside the wood is not easily discharged.

3.4 Porosity and pore size distribution

The removal of resin had a significant effect on wood porosity, which in turn affected the impregnation of wood. Table 3 shows the changes in the porosity of radiata pine sapwood and heartwood before and after the MS treatment. After the MS treatment, the total intrusion volume, total surface area, and porosity of radiata pine wood increased to varying

**Table 3** Automatic mercury porosimeter test results of wood before and after MW or MS treatment

Sample	Total Intrusion Volume (mL/g)	Total Surface Area (m²/g)	Mean Pore Diameter (nm)	Median Pore Diameter (nm)	Porosity (%)
S0	1.05	1.29	3260.7	6204.7	51.9
S-MS	1.15	3.02	1521	8347.7	54.6
H0	1.44	10.76	295.2	5343.6	63.9
H-MS	2.01	19.60	749.3	7490.5	71.3

Note: Control sapwood samples were recorded as S0, and MS-9 h as S-MS, control heartwood samples were recorded as H0, and MS-9 h as H-MS.

degrees. The total invasion volume of the sapwood control sample was 1.05 mL/g, and MS treatment increased the total invasion volume by 9.5%. The total invasion volume of the heartwood control sample was 1.44 mL/g, and the MS treatment increased the total invasion volume by 39.6%. The total invasion volume of heartwood was more significant than that of sapwood because heartwood contains more resin (Fig. 6) and the removal of resin can provide more pores. In addition, the increases in the total surface area, porosity, and median pore diameter of sapwood after MS treatment were 134.1%, 5.2%, and 34.5%, respectively,

whereas those of heartwood were 82.2%, 11.7%, and 40.2, respectively. However, the mean pore diameter of the sapwood decreased, while that of the heartwood increased.

The functional relationship between the rate of change in the pore volume and pore diameter is shown in Fig. 8. According to the anatomical structure, the diameter of the axial resin canal in pine radiata is 40–70 μm, the diameter of the radial resin canal is approximately one-third to one-fourth that of the axial resin canal, and the parenchyma cells are smaller (Cown 2011). Comparing Fig. 8a and b, the sapwood and heartwood of radiata pine differed in the entire pore size distribution range. The sapwood and heartwood pores were mainly distributed in 1–50 μm and 0.02–50 μm, respectively. After MS treatment, the porosity of the sapwood and heartwood increased to varying degrees. The most obvious change in sapwood was the notable increase in porosity at 15–50 μm, which may be due to the discharge of pine resin, resulting in more pores in the resin canal, parenchyma cells, and tubule cavity. Another change is that the pores near 5 μm decreased and developed into smaller pores, which may be due to the destruction of parenchyma cells; this part of the pores may have become larger, while the increase in pores near 1 μm may be due to the discharge
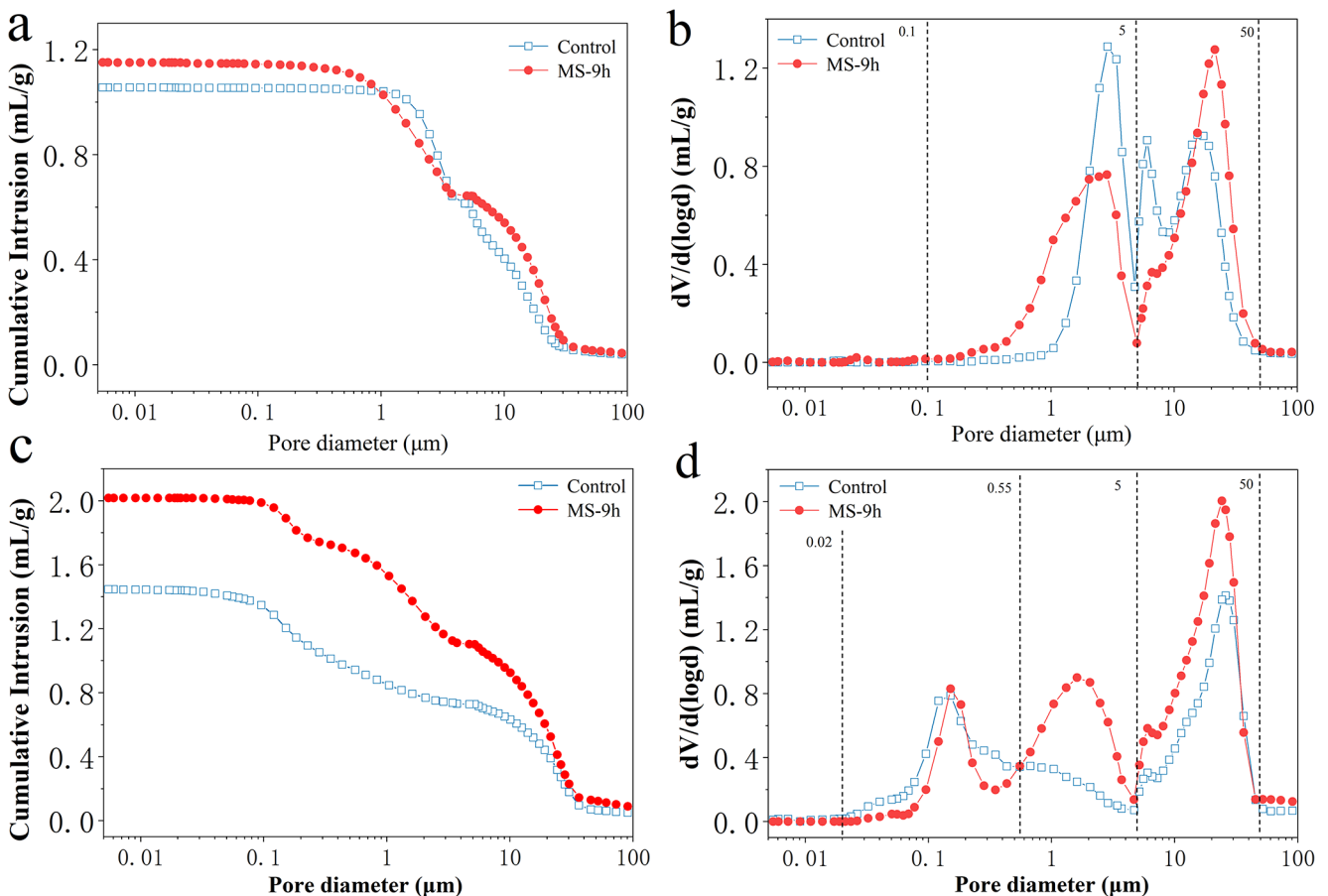
Fig. 8 Cumulative pore size distribution (**a**, **c**), pore volume change rate (**b**, **d**), and pore diameter of sapwood (**a**, **b**) and heartwood (**c**, **d**)

of resin or the destruction of the pit membrane by MS treatment (Weng et al. 2020). The porosity of the heartwood was increased in the range of 0.55–50 μm, which was larger. This is because heartwood contains more resin, and the MS treatment removes part of the resin from the resin canals and increases porosity. The increase in pores at 0.55–5 μm may be caused by the migration of oleoresin in latewood. The latewood of the radiated pine heartwood was almost completely filled with resin (Fig. 6b), whereas MS migrated to the resin (Fig. 6d). In addition, the pores did not change significantly in the range of 0.02–0.55 μm.

In summary, the MS treatment increased the porosity and pore size of radiata pine wood. There was a significant effect on the water uptake of wood, particularly in heartwood. Resin canals are the paths of liquid flow, and the discharge of the resin undoubtedly opens the penetration path and promotes liquid entry.

3.5 Water uptake

The uptake and toluidine blue penetration images of the radiata pine wood are shown in Fig. 9. Sapwood exhibited good water uptake, which is consistent with the results of a previous study (Matsumura et al. 1999). The uptake of the control samples exhibited no significant difference between the samples after MW, SS, and MS treatment, and the uptake range was 0.497 g/cm^3–0.583 g/cm^3. In addition, the liquid entered the interior of the wood in a radial manner and diffused to its surroundings (Fig. 9d), which is consistent with the results of previous studies. The liquid enters the interior of the wood through radial resin canals and ray cells and penetrates the surrounding tracheids (Matsumura et al. 1998).

The water uptake of heartwood was significantly lower than that of sapwood, the uptake rate of the untreated samples was low (0.045 g/cm^3–0.072 g/cm^3), and the dye solution was present only on the wood surface. After MW treatment, the uptake of heartwood increased to 0.121 g/cm^3–0.139 g/cm^3, and the uptake was more than double since, part of the resin on the surface layer was removed, which provided more paths for the dye solution to enter; however, the dye solution could not penetrate the interior of the wood, and only a small part of the area appeared to contain the dye solution (Fig. 9d) as the MW treatment could only remove

Fig. 9 Water uptake (a, b, c) and toluidine blue penetration images (d) of sapwood and heartwood
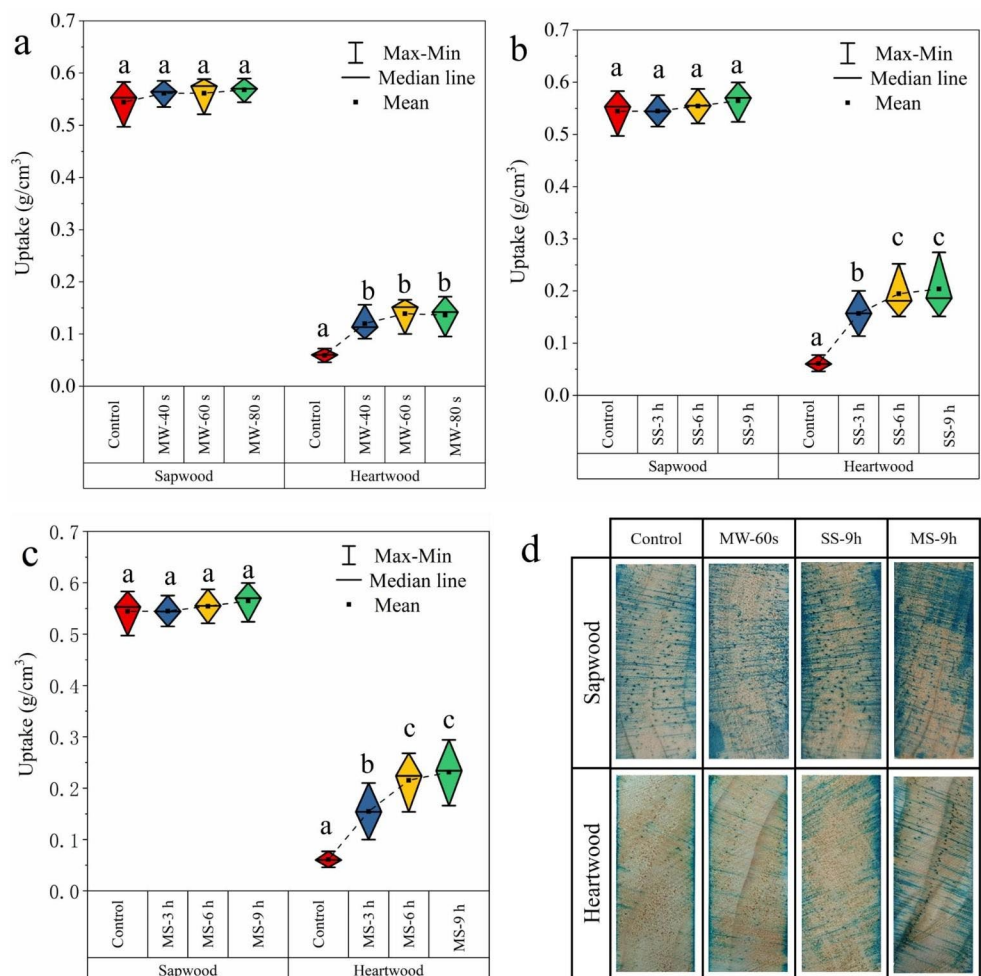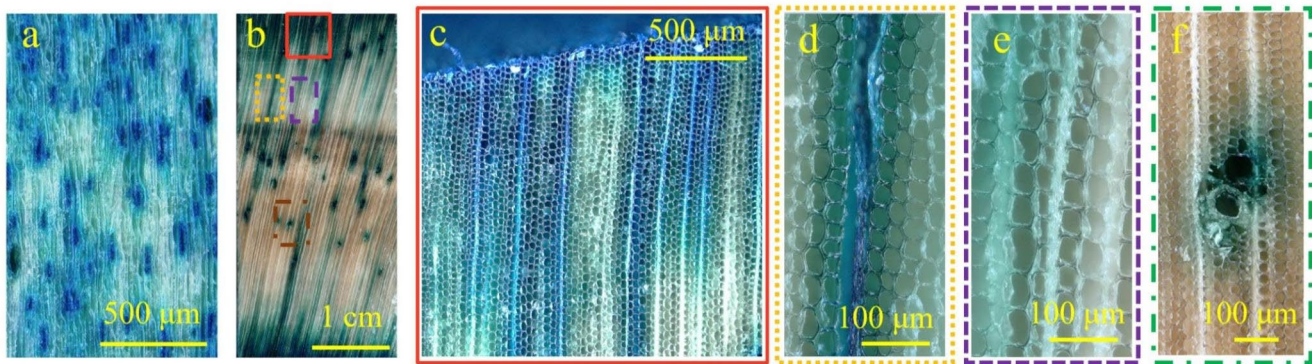
Fig. 10 Microscopic image of the heartwood MS-9 h sample after impregnation. (**a**) Tangential section; (**b**, **c**, **d**, **e**, and **f**) cross section, c, d, e, and f were locally enlarged images of b

part of the resin in the wood, and resin present in the resin canals blocked the penetration path of the liquid (Fig. 5b); therefore, the dye solution only entered the surface layer and the opened resin canals. After the SS treatment, the average uptake of the sample increased to approximately 0.121 g/cm³–0.139 g/cm³, and there were obvious traces of dye solution entering the cross-section (Fig. 9d). However, more than 50% of the parts still had no dye solution entering, which indicated that the resin canals or ray cells were not completely opened.

After MS treatment, the reduction in RC led to an increase in the uptake of the sample. Compared to the SS treatment samples, the average uptake of the MS treatment samples increased; however, the difference between the two groups of data was not significant, which may be due to the difference in wood variability. As shown in Fig. 8d, while more resin canals or ray cells are stained, the depth increases. This is because the MW treatment removed part of the resin and opened part of the resin canals, and further SS treatment continued to reduce the resin content. In addition, the planing treatment after the MW treatment prevented the resin from adhering to the wood surface to block the discharge of the resin; thus, the RC decreased further, the uptake increased, and the penetration depth increased. However, the uptake was still markedly lower than that of the sapwood, the penetration depth was shallower, and the amount of diffusion into the surrounding area was smaller, as the MS treatment did not completely remove the resin from the wood. In addition, the resin remaining in the resin canals or ray cells may hinder the diffusion of the dye solution to the surrounding areas, as rosin is also used as a hydrophobic agent in wood and bamboo (Dong et al. 2019; Su et al. 2021).

Figure 10 shows a microscopic image of heartwood MS-9 h samples. The resin canals and ray cells on the surface were infiltrated by the dye solution, whereas the surrounding tracheids were lighter in colour, indicating that the permeation path of the dye solution was consistent with that of sapwood, which is also a radial resin canal. Most of the

resin canals on the surface were penetrated by the dye solution, and the penetration of the dye solution was blocked as the depth increased (Fig. 10b, c). Further observation of the resin canal in the core revealed that the resin canal reached by the dye solution was larger, and the internal resin was partially removed (Fig. 10d), whereas the unstained resin canal was filled with resin (Fig. 10e). In addition, the axial resin canals were stained, even though they were in the core layer (Fig. 10f). This indicates that the radial and axial resin canals are interconnected, forming a resin canal network, which is the main pathway for fluid penetration (Matsumura et al. 1998). Under the conditions of this experiment, the treatment time was short and there was no pressure treatment; therefore, the uptake of the heartwood was low; however, it was more than thrice that of the untreated wood. Therefore, it can be used to improve the impregnation of radiata pine heartwood.

4 Conclusion

This study analysed the reasons for the improvement of the water uptake of radiata pine by MW and SS from the perspective of resin content. The results show that the water uptake of sapwood is outstanding. Although the MW, SS, and MS treatments reduced the resin content and increased porosity, they had no significant effect on the impregnation effect of sapwood. Heartwood was poorly permeable, and the control sample was almost impermeable. MW, SS, and MS treatments reduced the resin content and improved the impregnation effect of heartwood. Radial resin canals and rays are the main permeation paths of the tangential section, and the dye penetrates the wood through the open resin canals and rays. Thus, the MS treatment is a favourable strategy for increasing the water uptake of resinous wood and expanding its applications.

Declarations

Competing interests The authors declare no competing interests.

References

Aguayo MG, Oviedo C, Reyes L, Navarrete J, Gómez L, Torres H, Gaviño G, Trollund E (2021) Radiata pine wood treated with copper nanoparticles: leaching analysis and fungal degradation. Forests 12:1606. https://doi.org/10.3390/f12111606

Ai W, Duval H, Pierre F, Perré P (2017) Characterization of wood micromorphology from gas permeability measurements. Microfluid Nanofluid 21:101. https://doi.org/10.1007/s10404-017-1936-1

Ananías RA, Leandro-Zúñiga L, Pérez-Peña N, Salvo-Sepúlveda L, Cloutier A (2022) Transverse permeability in Eucalyptus nitens wood specimens. Wood Mater Sci Eng 1–8. https://doi.org/10.1080/17480272.2022.2102436

Andeme Ela RC, Chipkar SH, Bal TL, Xie X, Ong RG (2021) Lignin–propiconazole nanocapsules are an effective bio-based wood preservative. ACS Sustain Chem Eng 9:2684–2692. https://doi.org/10.1021/acssuschemeng.0c07742

Arbellay E, Stoffel M, Sutherland EK, Smith KT, Falk DA (2014) Resin duct size and density as ecophysiological traits in fire scars of Pseudotsuga menziesii and Larix occidentalis. Ann Botany 114:973–980. https://doi.org/10.1093/aob/mcu168

Bailey PJ, Preston RD (1969) Some aspects of softwood permeability. I. Structural studies with Douglas Fir sapwood and heartwood. Holzforschung 23:113–120. https://doi.org/10.1515/hfsg.1969.23.4.113

Bannan MW (1936) Vertical resin ducts in the secondary wood of the abietineae. New Phytol 35:11–46. https://doi.org/10.1111/j.1469-8137.1936.tb06864.x

Beikircher W, Lux C, Saxer A (2012) Microwave pretreatment of Norway spruce (Picea abies) for preservative treatment. Proceedings of the World Conference on Timber Engineering

Belt T, Keplinger T, Hänninen T, Rautkari L (2017) Cellular level distributions of Scots pine heartwood and knot heartwood extractives revealed by Raman spectroscopy imaging. Ind Crops Prod 108:327–335. https://doi.org/10.1016/j.indcrop.2017.06.056

Benedetti F, Rosales V, Opazo-Vega A, Norambuena-Contreras J, Jara-Cisterna A (2019) Experimental and numerical evaluation of hold-down connections on radiata pine cross-laminated-timber shear walls: a case study in Chile. Eur J Wood Prod 77:79–92. https://doi.org/10.1007/s00107-018-1365-1

Chen F, Gong AS, Zhu M, Chen G, Lacey SD, Jiang F, Li Y, Wang Y, Dai J, Yao Y, Song J, Liu B, Fu K, Das S, Hu L (2017) Mesoporous, three-dimensional wood membrane decorated with nanoparticles for highly efficient water treatment. ACS Nano 11:4275–4282. https://doi.org/10.1021/acsnano.7b01350

Cown DJ (2011) A review of resin features in radiata pine. N Z J Forest Sci 41:41–60

Dong Y, Zhang W, Hughes M, Wu M, Zhang S, Li J (2019) Various polymeric monomers derived from renewable rosin for the modification of fast-growing poplar wood. Compos Part B: Eng 174:106902. https://doi.org/10.1016/j.compositesb.2019.106902

Dong Y, Ji H, Dong C, Zhu W, Long Z, Pang Z (2020) Preparation of high-grade dissolving pulp from radiata pine. Ind Crops Prod 143:111880. https://doi.org/10.1016/j.indcrop.2019.111880

Eliseev SG, Ermolin VN, Stupnikov SS (2022) Using microwave irradiation to increase permeability of Siberian larch wood. IOP Conf Series: Mater Sci Eng 1230:012005. https://doi.org/10.1088/1757-899x/1230/1/012005

Fang X, Xiong Y, Li J, Ma X (2023) Treatability Changes of radiata pine heartwood induced by white-rot fungus trametes versicolor. Forests 14:1040. https://doi.org/10.3390/f14051040

Ganguly S, Balzano A, Petrič M, Kržišnik D, Tripathi S, Žigon J, Merela M (2021) Effects of different energy intensities of microwave treatment on heartwood and sapwood microstructures in Norway Spruce. Forests 12:558. https://doi.org/10.3390/f12050598

Hawley LF, Palmer RC (1912) Distillation of resinous wood by saturated steam. J Industrial Eng Chem 4:789–798. https://doi.org/10.1021/ie50047a003

He S, Chen C, Kuang Y, Mi R, Liu Y, Pei Y, Kong W, Gan W, Xie H, Hitz E, Jia C, Chen X, Gong A, Liao J, Li J, Ren ZJ, Yang B, Das S, Hu L (2019) Nature-inspired salt resistant bimodal porous solar evaporator for efficient and stable water desalination. Energy Environ Sci 12:1558–1567. https://doi.org/10.1039/C9EE00945K

Jang E-S, Kang C-W (2019) Changes in gas permeability and pore structure of wood under heat treating temperature conditions. J Wood Sci 65:37. https://doi.org/10.1186/s10086-019-1815-3

Jang E-S, Kang C-W (2023) An experimental study on efficient physical wood modification for enhanced permeability – focusing on ultrasonic and microwave treatments. Wood Mater Sci Eng 18:446–453. https://doi.org/10.1080/17480272.2022.2042852

Jiang F, Li T, Li Y, Zhang Y, Gong A, Dai J, Hitz E, Luo W, Hu L (2018) Wood-based nanotechnologies toward sustainability. Adv Mater 30:1703453. https://doi.org/10.1002/adma.201703453

Kang C-W, Kolya H, Jang E-S, Zhu S, Choi B-S (2021) Steam exploded wood cell walls reveals improved gas permeability and sound absorption capability. Appl Acoust 179:108049. https://doi.org/10.1016/j.apacoust.2021.108049

Li X, Zhang B, Li W, Li Y (2005) Research on the effect of microwave pretreatment on moisture diffusion coefficient of wood. Wood Sci Technol 39:521–528. https://doi.org/10.1007/s00226-005-0007-z

Mahdian M, Huang LY, Kirk DW, Jia CQ (2020) Water permeability of monolithic wood biocarbon. Microporous Mesoporous Mater 303:110258. https://doi.org/10.1016/j.micromeso.2020.110258

Matsumura J, Booker RE, Donaldson LA, Ridout BG (1998) Impregnation of radiata pine wood by vacuum treatment: identification of flow paths using fluorescent dye and confocal microscopy. IAWA J 19:25–33. https://doi.org/10.1163/22941932-90000649

Matsumura J, Booker RE, Ridout BG, Donaldson LA, Mikajiri N, Matsunaga H, Oda K (1999) Impregnation of radiata pine wood by vacuum treatment II: effect of pre-steaming on wood structure and resin content. J Wood Sci 45:456–462. https://doi.org/10.1007/BF00538953

Nguyen TTH, Li S, Li J, Liang T (2013) Micro-distribution and fixation of a rosin-based micronized-copper preservative in poplar wood. Int Biodeterior Biodegrad 83:63–70. https://doi.org/10.1016/j.ibiod.2013.02.017

Pakowski Z, Adamski R, Kokocinska M (2009) Cross-fiber dry wood darcy permeability of energetic willow salix viminalis v. Orm. Drying Technol 27:1379–1383. https://doi.org/10.1080/07373930903383653

Pokki J-P, Laakso VV, Tikka P, Aittamaa J (2010a) Specific permeability of wood to water part 1: longitudinal specific permeability of steamed, impregnated, and kraft-cooked wood. Ind Eng Chem Res 49:2144–2154. https://doi.org/10.1021/ie801901f

Pokki J-P, Laakso VV, Tikka P, Aittamaa J (2010b) Specific permeability of wood to water part 2: perpendicular specific permeability of steamed, impregnated, and kraft-cooked wood. Ind Eng Chem Res 49:2155–2160. https://doi.org/10.1021/ie801902b

Potter FS, Schuerch C (1975) An industrial steam distillation: separation of rosin and turpentine from pine gum. J Chem Educ 52:672. https://doi.org/10.1021/ed052p672

Qian HE, Hou Q, Hong L, Lu X, Ziegler-Devin I, Chrusciel L, Besserer A, Brosse N (2022) Effect of highly efficient steam explosion treatment on beech, poplar and spruce solid wood physicochemical and permeable performances. Ind Crops Prod 182:114901. https://doi.org/10.1016/j.indcrop.2022.114901

Singh R, Krishna BB, Kumar J, Bhaskar T (2016) Opportunities for utilization of non-conventional energy sources for biomass pretreatment. Bioresour Technol 199:398–407. https://doi.org/10.1016/j.biortech.2015.08.117

Srinivasan N, Bhattacharyya D, Jayaraman K (2007) Thermoforming of wood veneer composite sheets. 61:558–562. https://doi.org/10.1515/HF.2007.105

Su N, Fang C, Zhou H, Tang T, Zhang S, Fei B (2021) Hydrophobic treatment of bamboo with rosin. Constr Build Mater 271:121507. https://doi.org/10.1016/j.conbuildmat.2020.121507

Taghiyari HR, Habizade S, Miri Tari SM (2014) Effects of wood drying schedules on fluid flow in Paulownia wood. Drying Technol 32:89–95. https://doi.org/10.1080/07373937.2013.813855

Tan Y, Hu J, Chang S, Wei Y, Liu G, Wang Q, Liu Y (2020) Relationship between pore structure and gas permeability in poplar (Populus deltoides CL.'55/65') tension wood. Ann for Sci 77:88. https://doi.org/10.1007/s13595-020-00994-6

Torgovnikov G, Vinden P (2010) Microwave wood modification technology and its applications. For Prod J 60:173–182. https://doi.org/10.13073/0015-7473-60.2.173

Vinden P, Torgovnikov G, Hann J (2011) Microwave modification of radiata pine railway sleepers for preservative treatment. Eur J Wood Prod 69:271–279. https://doi.org/10.1007/s00107-010-0428-8

Washburn EW (1921) Note on a method of determining the distribution of pore sizes in a porous material. Proc Natl Acad Sci 7:115–116. https://doi.org/10.1073/pnas.7.4.115

Weng X, Zhou Y, Fu Z, Gao X, Zhou F, Fu F (2020) Effects of microwave treatment on microstructure of Chinese fir. Forests 11:772. https://doi.org/10.3390/f11070772

Weng X, Zhou Y, Fu Z, Gao X, Zhou F, Jiang J (2021) Effects of microwave pretreatment on drying of 50 mm-thickness Chinese fir lumber. J Wood Sci 67:13. https://doi.org/10.1186/s10086-021-01942-2

Wu HX (2019) Review of the book 'Domestication of radiata pine'. Australian Forestry 82:48–51. https://doi.org/10.1080/00049158.2019.1578451

Zhang Y, Lin L, Fu F (2021) High-permeability wood with microwave remodeling structure. Forests 12:1432. https://doi.org/10.3390/f12111432